Comparative study of pure and Co-doped $BaFe_2As_2$

Jacques Soullard,[1,*] Raul Perez-Enriquez,[2,†] and Ilya G. Kaplan[3,‡]
[1]*Instituto de Física, UNAM, Apartado Postal 20-364, 01000 Mexico DF, Mexico*
[2]*Departamento de Estado Sólido, Universidad de Sonora, Mexico*
[3]*Instituto de Investigación en Materiales, UNAM, Apartado Postal 70-360, 04510 Mexico DF, Mexico*
(Received 5 December 2014; revised manuscript received 27 February 2015; published 28 May 2015)

We present a comparative calculation of the electronic structure of the high critical temperature superconductor Co-doped $BaFe_2As_2$ and its parent compound at the electron correlation level by the embedded cluster method; the electron correlation is calculated through the second-order Møller-Plesset perturbation theory. The superconducting doped material is represented by the $Ba_4CoFe_4As_8$ cluster. The analysis of the orbital populations in this cluster reveals the formation of an antiferromagnetic order in the Fe plane with a spin-density increase on the central Co atom with respect to the spin density of the central Fe atom of the undoped case. This increase is associated with an increase of the d_{z^2} orbital population of the central atom. However, the formation mechanism of the local magnetic moment implies also a spin transfer from the nearest-neighbor Fe atoms and from the next-nearest-neighbor As atoms to the central Co atom, and it corresponds to a J_1-J_2 antiferromagnetic Heisenberg model. Some particular features of d_{yz} and $d_{x^2-y^2}$ orbitals in the triplet and in the singlet cluster states are interpreted to correspond to a spinless fermion. This result, as well as the result relative to the formation mechanism of the magnetic moments, can be connected with a model of resonating-valence-bond (RVB) superconductors suggested recently by Poilblanc *et al.* [Phys. Rev. B **89**, 241106 (2014)] and based on the Anderson RVB theory.

DOI: 10.1103/PhysRevB.91.184517 PACS number(s): 74.20.Pq, 71.15.Ap, 36.40.Cg, 74.70.Xa

I. INTRODUCTION

Iron pnictides are the latest family of high critical temperature superconductors discovered [1,2]. If iron chalcogenides are included, we have six groups of iron-based compounds that present superconductivity with a high critical temperature: (i) 1111 materials such as RFeAsO (where R is a rare earth) superconducting (SC) under electron doping; (ii) 122 materials such as AFe_2As_2 (with A = Ca, Sr, Ba, or Eu) SC under hole doping in the plane of A atoms or under substitution of Fe by Co or Ni (electron doping); (iii) 111 material AFeAs (A = Li,Na); (iv) 11 materials such as FeTe or $Fe(Se_{1-x}Te_x)$; (v) 122$*$ defective compounds $A_xFe_{2-y}Se_2$ (A = K,Rb,Cs,Tl), and (vi) the 2131 family Sr_2MO_3FePn, with M = Sc and Pn = As or M = V and Pn = P (see Ref. [3]).

The most studied of these groups is the Ba-based 122 system for the availability of large and high-quality single crystals suitable for experiments and for the possibility to produce SC materials on a variety of chemical doping. The undoped material is a paramagnetic semimetal at room temperature that undergoes structural and magnetic transitions at 140 K [4]; the tetragonal-to-orthorhombic transition is associated with the onset of antiferromagnetic (AFM) order [5,6]. The study of magnetic excitations through inelastic neutron scattering allows to determine a fluctuating magnetic moment, $\langle m^2\rangle = 3.2\mu_B^2$ [7]. The substitution of either the alkaline-earth (Ba), the transition metal (Fe), or the pnictogen (As) atom with different elements produces generally a superconducting phase. However, the SC phase is sensitive to the particular choice of ion substituent. In 122-type materials, superconductivity, first shown to occur by Co substitution of Fe in $SrFe_2As_2$ [8] and $BaFe_2As_2$ [9], it is stabilized also by several types of d-metal substitution. This includes the use of any elements in the Ni, Co, and Fe column (except, so far, Os) (see Ref. [10] and references therein), but it excludes Cr [11], Mo [12], Mn [13], and Cu [14,15], which act to suppress magnetism without stabilizing the high-T_C SC phase. It is not clear yet why Co and Ni located on the electron-doping side of Fe produce a SC state, while Mn, Cr, and Mo located on the hole-doping side do not. Isovalent doping (substitution of Fe by Ru [16]) also gives rise to superconductivity; a distinction has to be made between charge doping and chemical substitution (Ru).

Soon after the discovery of the Fe SC, density-functional-theory (DFT) calculations revealed the main features of the electronic structure of doped and undoped $BaFe_2As_2$. It was shown that they have a quite complicated band structure and several disconnected Fermi surfaces (FSs) [17,18]. All five $3d$ orbitals of Fe are involved in the electronic structure of FSs. There are two types of FSs: three-hole FSs are located in the center of the Brillouin zone, and two-electron FSs are located at the corner. In theoretical studies [18–20], the magnetic nature of superconductivity in FeSCs was suggested.

While transport experiments [21], optical spectroscopy [22], Raman spectroscopy [23], neutron-diffraction experiments [24], and angle-resolved photoelectron spectroscopy (ARPES) [25–29] are qualitatively in agreement with these theoretical results, quantitative discrepancies exist between experimental and theoretical results. For instance, in AFe_2As_2 (A = Ba,Ca,Sr), the magnetic moments estimated from neutron scattering experiments [6,30,31] on Fe to be in the range of 0.8–1.0 μ_B, whereas DFT calculations give 1.6–1.9 μ_B [32]. This kind of discrepancy is not particular to 122 compounds, but it is common to other ferropnictides such as LaFeAsO [32].

*soullard@fisica.unam.mx
†rpereze@correo.fisica.uson.mx
‡kaplan@iim.unam.mx

At present in many theoretical studies (see, for example, [18,19] and the reviews [20,33,34]), it is accepted that Fe SCs possess nonconventional superconductivity with an electron-pairing mechanism that has not been realized yet. Calculations of magnetic susceptibility [18] showed that these new superconducting materials have a tendency to form AFM order, and the wave vectors associated with the spatial periodicity of the magnetic moments coincide with those connecting the centers of the electron and hole FSs. Based on this, Mazin *et al.* [18] proposed that AF spin fluctuations can induce s-wave pairing with sign reversal of the order parameter between electron- and holelike FSs; this kind of pairing is denoted as $s_{\pm}$. The latter was obtained also in Ref. [19], while the authors [19] did not exclude the d-wave pairing as a possible candidate. The tendency toward magnetism existing at zero doping is suppressed by AF spin fluctuations.

In most theoretical studies (see [35–37]), it follows that Fe SCs can be considered as doped Mott insulators with effective nearest-neighbor (nn) and next-nearest-neighbor (nnn) antiferromagnetic exchange interaction. In this model, antiferromagnetism [35,36] and $s_{\pm}$ pairing [36,37] are also revealed. It should be mentioned that, as discussed in Ref. [38], the Anderson resonating valence bond (RVB) state of high-temperature superconductivity can be naturally applied in the Mott insulator model. Anderson [39] proposed his RVB model for high-temperature superconductors just after the discovery of copper superconductors. According to Anderson, in the RVB state the antiferromagnetic (Néel) lattice will be melted into a spin-liquid phase consisting of singlet pairs. Upon carrier doping, these singlets would become charged, resulting in the SC state. Basing on the so-called "separation of charge and spin," the electronic excitation spectra in the RVB state can be presented as two separated branches: charge spinless holons and chargeless spinons [40,41]; see also the discussion between Anderson and Schrieffer in Ref. [42].

Recently, Anderson's RVB ideas were applied by Poilblanc *et al.* [43] to construct a family of fermionic projected entangled pair states on a square lattice. They showed that under doping, the insulating RVB spin liquid evolves into a superconducting state with mixed $d + \imath s$ pairing symmetry, where the relative weight between s and d components is controlled by a variational parameter c. Optimizing the hole kinetic energy with respect to c, Poilblanc *et al.* [43] obtained a sufficiently good description of the frustrated spin-1/2 J_1-J_2 AFM Heisenberg model proposed earlier for iron pnictide superconductors [44,45]. The orbital symmetry of the optimized RVB superconductor has predominant d-wave character.

However, the results of an analysis of photoinduced transient changes of the mid-infrared conductivity in the SDW state and in the normal state (slightly above T_{SDW}), obtained through pump-probe spectroscopy of $BaFe_2As_2$, attest to a pronounced spin-phonon coupling that may play a role in the formation mechanism of SDW and in the superconducting states of pnictides [46]. The spin-phonon coupling is in accord with the existence of a strong magnetoelastic effect revealed by high-resolution x-ray-diffraction measurements in $BaFe_{2-x}Co_xAs_2$ [47,48]. Nevertheless, the evolution with temperature and pressure of the optical conductivity of the parent compound and its comparison with that found upon doping indicate that the lattice modifications cannot be recognized as the only parameter determining the electrodynamics in these compounds [49].

Indeed, optical conductivity obtained in an infrared optical study of these compounds is related to electronic correlation. From an analysis of the spectral weight transfer in these moderately strong correlated electron materials, Hund's coupling is assumed to be the primary mechanism responsible for electron correlation [50]. Accordingly, iron-based superconductors are considered as Hund's correlated metals [51]. Electron correlation in iron-based superconductors is discussed in a review [52]. From this study, it follows that the ratio of the experimental kinetic energy and the kinetic energy from band theory [local density approximation (LDA)] has a value below unity for correlated metals and almost equal to unity for conventional metals (in the case of $BaFe_2As_2$, this value is about 0.3 [52]). As pointed out by the authors of [52], the central point of electron correlation is the interplay between the itinerancy of electrons in solids and localizing effects generally rooted in electron-electron repulsion.

Furthermore, undoped $BaFe_2As_2$ exhibits a single structural/magnetic transition [53] that splits into two distinct phase transitions, both of which are suppressed when the Co concentration increases. The SC phase appears when the Co concentration is greater than a critical concentration at about $x \geqslant 0.038$ [53,54]. At this low Co concentration x, the AFM phase and the SC phase coexist. However, at higher concentration, a magnetic transition occurs and a nematic phase appears [55], but the crystal is still SC with an orthorhombic structure [56,57]. The nematic electronic liquid crystal state is one of the consequences of strong electron correlation. The two transition lines – magnetic and nematic – penetrate separately in the superconducting dome. Deep in the superconducting dome ($T = 0$ K), these two lines merge in a quantum phase transition [58]. Beyond $x = 0.06$, the tetragonal/orthorhombic transition as well as the nematic/paramagnetic transition are completed, and the SC critical temperature reaches its maximum (23 K) at the Co concentration $x = 0.074$ [53]. See Fig. 1 of this paper (taken from [57]) and Fig. 1 of Ref. [58] for the part of the phase diagram at low temperature where there is no experimental data.

In this paper, we present a comparative study of the electronic structure of pure and Co-doped $BaFe_2As_2$ oriented to contribute to the discussion of some of the points described above. We study pure $BaFe_2As_2$ and then the Co-doped material at low Co concentration in the orthorhombic phase when it is SC with AFM order and when it becomes SC in the absence of magnetism but still in the orthorhombic phase; there is an experimental ARPES study of this transition known as a Lifshitz transition [27]. We have employed the electron-correlated embedded cluster method (ECM − MP2) developed by our group [59–62]. In this method, the selected cluster is embedded in the Madelung field of the crystal. The orbital population is first calculated at the Hartree-Fock (HF) level. Then, the correlation correction to the HF result is calculated through the second-order Møller-Plesset (MP2) perturbation theory (PT); see the presentation of this PT and its relation with HF calculations in Appendix 3 of Ref. [63], or the alternative presentation from the viewpoint of a

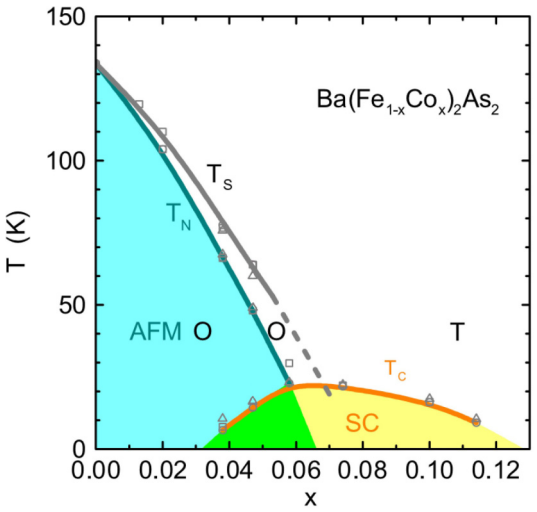

FIG. 1. (Color online) Phase diagram of the $Ba(Fe_{1-x}Co_x)_2As_2$ superconductor showing paramagnetic tetragonal (T), paramagnetic orthorhombic (O), AFM ordered orthorhombic (AFM O), and superconducting (SC) phases (from Ref. [57]).

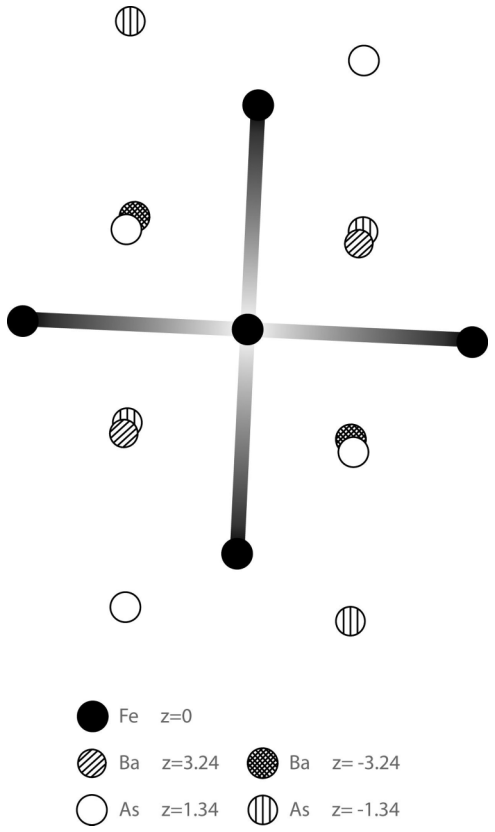

FIG. 2. Cluster $Fe_5As_8Ba_4$ (units of Å).

many-body perturbation theory in the context of molecular cluster computations [64].

II. METHODOLOGY

The ECM-MP2 methodology includes two parts: (i) a method for a quantum-mechanical calculation of the electronic structure of the cluster that takes into account electron correlation; and (ii) an embedding scheme to couple the cluster to its environment, which represents an infinite crystal. Details of the methodology are given in Refs. [59–62]. The purpose of the embedding scheme is to reproduce the Madelung potential of the infinite crystal on each site of the cluster of atoms that represents the material under study. This is achieved by adjusting the external charges of a finite array of point charges that embeds the cluster. The determination of the cluster charge as well as the background charges depend on the bonding that characterizes the material under study. For metals, the simple ionic charges or those obtained from DFT calculations are usually used.

As $BaFe_2As_2$ is a semimetal, the cluster charge is given from the Löwdin charges obtained from a calculation of the electronic structure within DFT using the QUANTUM ESPRESSO package [65]. The plane-wave DFT calculations [66] were performed at the local spin density approximation (LSDA), then the exchange-correlation potential of Perdew-Burke-Ernzerhof (PBE) was applied. To model the electronic interactions with inner shells, we used the ultrasoft pseudopotentials $As.pbe\text{-}n\text{-}rrkjus_psl.0.2.UPF$, $Ba.pbe\text{-}nsp\text{-}van.UPF$, and $Fe.pbe\text{-}nd\text{-}rrkjus.UPF$ from http://www.quantum-espresso.org. The structural information on the system under investigation is taken from Ref. [4]; the spin-polarized calculation was started with a magnetization of $-0.2\mu_B$ on the central Fe and $0.7\mu_B$ on Fe in the other plane; the cutoff energy for wave functions is 50 eV, while that for charge density and potential is 250 eV. The wave functions obtained in the previous DFT calculations are projected onto the orthogonalized orbitals of the pseudopotentials to obtain the Löwdin charges and the magnetic moments on each Fe atom. They were found to be equal to $-2.19\mu_B$ for the central Fe and $2.22\mu_B$ for the other Fe atoms. The Löwdin charges for Ba, Fe, Fe (central), and As are, respectively, -0.45, 0.52, 0.49, and -0.16.

These charges are not consistent with a neutral unit cell and with the fact that we require an odd integer cluster charge to simulate a magnetic structure in our calculation of the pure $BaFe_2As_2$ represented by the cluster $Fe_5As_8Ba_4$ (Fig. 2). Therefore, they were readjusted to fulfill the two above-mentioned requirements. The new charges are -0.61, 0.33, and -0.023 for Ba, Fe, and As, respectively; they give a cluster charge $q = -1$. These charges are the initial charges of an iterative calculation to obtain background charges that produce convergent set of charges.

The cluster $Ba_4Fe_5As_8$ with its charge $q = -1$, chosen to represent the ternary iron arsenide $BaFe_2As_2$ in the present work, is appropriated to study the modifications of the electronic structure upon substitution of the central Fe by another transition metal (Co). Indeed, it is associated with a magnetic structure, and its symmetry properties are also adequate. They are given by the point group D_2, a subgroup of the space group $Fmmm$ (D_{2h}^{23}) of the $BaFe_2As_2$ crystal that belongs to the orthorhombic system. We take into account the experimental crystallographic data of the structure given in Ref. [4].

With respect to the background charges, we have to solve the following problem: the background charges derived from the cluster ion charges obtained after a quantum-mechanical

calculation are different from the previous background charges. However, consistency between two sets of background charges is obtained after a series of quantum calculations in which the cluster charges obtained from a previous calculation are taken to calculate a new set of background charges; this process also makes the sets of cluster charges (calculated quantum mechanically) consistent. At each step of the iteration procedure, the unit cell neutrality and the cluster charge are preserved (see Ref. [60] for a detail description of the procedure). In our case, the final background charges are 0.0138, 0.333, and −0.3402 for Ba, Fe, and As, respectively, starting from the charges given above.

The *ab initio* quantum cluster calculations were performed with the GAUSSIAN-09 program [67]. The background charges are introduced in the quantum calculation through the keyword CHARGE. For Fe and As, all electrons were taken into account with the standard triply split valence basis sets 6-311$G(d)$ for Fe and 6-311G for As. For the Ba atoms, the core electrons were included in the Wood-Boring pseudopotential (MWB46), and the associated basis set was used for the valence electrons. In these conditions, the natural bond orbital (NBO) analysis could be used to calculate the charges on atoms and the orbital populations. The correlation correction to the HF result calculated at the MP2 level takes into account all molecular orbitals (GAUSSIAN09 keyword MP2Full). This approach avoids a failure of the MP2 calculation due to an excessive mixing of frozen core orbitals and valence orbitals. This approach differs from the (Default) MP2 calculations that freeze the core molecular orbitals.

III. RESULTS AND DISCUSSION

In the nonrelativistic approximation, the Hamiltonian does not depend on the spin. In this approximation for clusters of atoms, as for polyatomic molecules, the operator for the square of the total spin angular momentum ($\mathbf{S}^2$) commutes with the electronic Hamiltonian. Therefore, the electronic terms of the cluster are classified according to the multiplicity. In our case, the $Fe_5As_8Ba_4$ cluster with charge $q = -1$ has an odd number of electrons, so we report in Table I(a) the cluster energies for states with one, three, five, or seven unpaired electrons with multiplicity $M = 2, 4, 6$, or 8, respectively. The cluster energy is obtained when the self-energy of the background charges is subtracted from the energy of the charge array (cluster plus background charges); both are given by the Gaussian program. We report the eigenvalues of the $\mathbf{S}^2$ operator before the first annihilation of the spin contaminant; the values when the spin contaminant is removed are indicated in parentheses. Thus, we can appreciate that the spin states are well-defined.

TABLE I. Cluster energy calculated by the ECM-MP2 method.

Multiplicity	Energy (a.u.)	$\mathbf{S}^2$	($\hbar^2$)
	(a) $Fe_5As_8Ba_4$		
2	−24293.26215	2.10	(1.97)
4	−24293.25282	3.87	(3.75)
6	−24293.26702	8.98	(8.76)
8	−24293.21967	15.92	(15.76)
	(b) $CoFe_4As_8Ba_4$		
1	−24412.3754643	0.0	
3	−24412.2964173	3.31	(2.71)
5	−24412.2963723	6.13	(6.00)
7	−24412.2872351	12.19	(12.00)

The ground state of the undoped cluster corresponds to a spin state with multiplicity $M = 6$. In the doublet state there is a very high spin contamination (we obtain a spin value $S = 1$ instead of $S = 1/2$). This unsatisfactory result is not taken into account because it is not related to the ground state. For the Co-doped cluster, we report four states: the first one (the singlet state) allows us to study the nonmagnetic structure of doped-$BaFe_2As_2$, while the second one (the triplet state) allows us to study the AFM and SC structure. The background charges are the same as those used to obtain the cluster charges for the undoped material. In both cases, the cluster charge is $q = -1$, and the electron number of the doped cluster is thus even.

A. The undoped cluster

In this section, we present the results obtained for the undoped cluster in the ground state (the sextet state), which characterizes the electronic structure of the pure $BaFe_2As_2$ material. This is the reference state that will be used to give evidence of the effects of doping by Co atoms.

The charge on atoms and the valence orbital population obtained at the MP2 level for pure $BaFe_2As_2$ are presented in Table II. Only the central atom of the cluster, its nearest neighbor (n.n.) Fe, and its next-nearest neighbor (n.n.n.) As are considered; the results relative to the external As and Ba atoms of the cluster, which are in an environment of symmetry different from D_2, are not reported. The small populated excited orbitals corresponding to Rydberg states as well as the populations of $4p$(Fe) atoms, which are always small, are not reported, but their population is taken into account in the final values of atomic charges (second column of Table II).

The results show an overall symmetry consistent with the D_2 point group. With respect to the orbital population of the free atoms, the valence orbital population in crystal shows a strong population decrease on the $4s$(Fe) orbitals and a corresponding increase of the $4p$(As) orbital population; there is also an increase of the $3d$(Fe) orbital population of $0.6e$ for the central Fe and the Fe atoms along the a axis of the crystal structure (denoted Fe-a). For the Fe ions along the b axis (Fe-b), this increase is smaller (only $0.48e$) and the decrease of their $4s$ orbital is also less. Some $3d$(Fe) orbitals are completely filled; they are doubly occupied and the resulting spin density is zero. This is the case for the $3d_{xy}$, $3d_{xz}$, and $3d_{yz}$ orbitals of the central Fe and for the $3d_{xy}$ and $3d_{z^2}$ orbitals of Fe-a. The other $3d$ orbitals are partially filled.

In respect to spin density, $3d_{z^2}$(Fe) contributes mainly to the spin density on the central Fe; the contribution of the $3d$ orbitals to the spin density on Fe-b comes mainly from the electron of the $3d_{yz}$ orbital (its charge density is equal to $1e$). The other contribution to the spin density on Fe-b comes from the $4s$ orbital. The sum of the contributions of the $4s$ and $3d$ orbitals to the spin density of Fe-a is practically zero; we note only a small contribution of opposite sign from $3d_{yz}$ and $3d_{x^2-y^2}$. The $4p$ population of the "insulating" As atoms

TABLE II. Charge and spin distribution at the MP2 level (NBO analysis) in a pure $Fe_5As_8Ba_4$ cluster ($S = 5/2$).

	Charge spin	Valence orbital population	Detailed charge and spin population on $3d$(Fe) and $4p$(As) orbitals
		(a) charge distribution	
Fe	0.82	$4s^{0.46}3d^{6.61}$	$d_{xy}^{1.91} + d_{xz}^{1.95} + d_{yz}^{1.87} + d_{x^2-y^2}^{0.39} + d_{z^2}^{0.48}$
Fe(n.n.)-*a*	0.76	$4s^{0.49}3d^{6.65}$	$d_{xy}^{1.72} + d_{xz}^{0.68} + d_{yz}^{0.67} + d_{x^2-y^2}^{1.67} + d_{z^2}^{1.91}$
Fe(n.n.)-*b*	0.51	$4s^{0.91}3d^{6.48}$	$d_{xy}^{0.89} + d_{xz}^{1.49} + d_{yz}^{1.02} + d_{x^2-y^2}^{1.61} + d_{z^2}^{1.47}$
As(n.n.n.)	−1.13	$4s^{1.74}4p^{4.34}$	$p_x^{1.41} + p_y^{1.56} + p_z^{1.37}$
As(n.n.n.)	−1.13	$4s^{1.74}4p^{4.34}$	$p_x^{1.41} + p_y^{1.56} + p_z^{1.37}$
		(b) (α-β) spin distribution	
Fe	0.31	$4s^{0.01}3d^{0.30}$	$d_{xy}^{-0.02} + d_{xz}^{0.00} + d_{yz}^{0.08} + d_{x^2-y^2}^{-0.02} + d_{z^2}^{0.27}$
Fe(n.n.)-*a*	0.08	$4s^{0.00}3d^{0.08}$	$d_{xy}^{0.00} + d_{xz}^{0.02} + d_{yz}^{0.11} + d_{x^2-y^2}^{-0.09} + d_{z^2}^{0.04}$
Fe(n.n.)-*b*	0.41	$4s^{0.23}3d^{0.18}$	$d_{xy}^{0.10} + d_{xz}^{-0.10} + d_{yz}^{0.25} + d_{x^2-y^2}^{-0.05} + d_{z^2}^{-0.02}$
As(n.n.n.)	0.11	$4s^{0.02}4p^{0.09}$	$p_x^{0.08} + p_y^{-0.03} + p_z^{0.04}$
As(n.n.n.)	0.11	$4s^{0.02}4p^{0.09}$	$p_x^{0.08} + p_y^{-0.03} + p_z^{0.04}$

increases by 1.34*e*, but their 4*s* orbitals lose 0.26*e*, and the spin density on these orbitals is small.

Therefore, we have magnetic moments along the *b* axis of the crystal. This is not in contradiction with the AFM order observed in this material in the *c* direction, because we have only one Fe plane. The ferromagnetic alignment along the **b** axis and the AFM order along the **c** axis are also observed in the experimental work of Huang *et al.* [5]. They measured a magnetic moment of $0.87\mu_B$ on Fe similar to our calculated moment 0.51–0.82 μ_B. On the other hand, in our calculation there is no AFM order along the **a** axis as detected experimentally in Ref. [6].

We want to point out an asymmetry in our results: the orbital occupation of $3d_{xz}$ and $3d_{yz}$ on the *b* axis is greater than the occupation of the same orbitals on the *a* axis. From this unequal occupation of $3d_{xz}$ and $3d_{yz}$, a so-called orbital order occurs [68–71]. This orbital order is assumed to be the underlying cause of anisotropies observed in many experiments, including optical [72,73], resistivity, and magnetoresistance measurements [74,75], and a variety of spectroscopic measurements, such as ARPES [76,77]. The in-plane electronic asymmetry is not connected in particular to $BaFe_2As_2$, but it is common to underdoped 122-Fe arsenide superconductors; see Ref. [78].

Our results reinforce the hypothesis that the anisotropy observed in 122 iron pnictides results from orbital ordering. On the other hand, our method cannot give any information relative to the alternative hypothesis: namely, the dopant-induced transport anisotropy in 122 iron pnictides is due to the formation of magnetic unidirectional nematogens, which are formed by the impurity, and exhibit a dimer structure whose length is about 10 lattice constants [79,80]. The size of this structure is greater than our cluster size, so it cannot be detected using our method.

B. The Co-doped cluster in the triplet state

The properties of the Co-doped $Fe_5As_8Ba_4$ cluster in the triplet state are expected to provide relevant information on orthorhombic $BaFe_2As_2$ characterized by an AFM order and superconductivity at low temperature. As follows from Table I(b), the magnetic ground state for the Co-doped cluster with multiplicities 3 and 5 is practically degenerated.

The atomic charge densities in the Co-doped material are not very different from those in the pure material (see Table III). The Co atom occupies the central position; it keeps its additional electron (with respect to the Fe atom) and attracts an additional electron density of 0.35*e*. This small additional density comes from the neighboring Fe atoms; therefore, their individual charge densities are practically unchanged. There is also a small increase ($\sim 0.1e$) of the $4p_x(As)$ and $4p_z(As)$ orbital population that increases the anionic charge of As.

If the charge densities are not notably affected by the Co doping, we note on the contrary a strong modification of the spin distribution. The spin density on the Co atom is now almost unity (more than three times the spin density of the central Fe in the case of the pure material); the sign of the spin density on Fe-*b* and As is reversed, and its magnitude is diminished on the Fe and As atoms. Thus, there is a spin transfer to the central Co atom from its neighbors. It is known from NMR experiments that Co doping clearly modifies the magnetic ordering of $BaFe_2As_2$ [81].

We can get more insight into these effects by looking at the spin orbital populations. The doubly occupied orbitals of the pure material keep their double occupancy with a null spin density, and the modification consists in a redistribution of the spin density among the partially filled orbitals. The spin of the Co atom is attributed to the single electron of the $3d_{z^2}$(Co) orbital; its charge density is practically 1*e* and its spin density practically unity. The negative spin density on the Fe-*b* ion is associated with the $4s$(Fe-*b*) orbital spin density, which is now −0.21 instead of 0.23 in the pure state. The contribution of the $3d$(Fe-*b*) orbital population becomes practically zero (−0.06), while it was equal to 0.18 in the pure state. From these two facts, AFM order results along the *b* axis of the crystal structure. The $3d$(Fe-*a*) orbitals produce nearly null spin densities that explain the decrease of the spin density on Fe-*a*. The Co impurity acts in a similar way on the $4s$(As) orbitals. The spin direction is opposite to that of the pure material, and the spin density is also diminished; there is no

TABLE III. Charge and spin distribution at the MP2 level (NBO analysis) in Co-doped $Fe_5As_8Ba_4$ cluster ($S = 1$).

	Charge spin	Valence orbital population	Detailed charge and spin population on $3d$(Fe) and $4p$(As) orbitals
		(a) charge distribution	
Co	1.03	$4s^{0.48}3d^{7.35}$	$d_{xy}^{1.94} + d_{xz}^{1.95} + d_{yz}^{1.96} + d_{x^2-y^2}^{0.33} + d_{z^2}^{1.18}$
Fe(n.n.)-a	0.80	$4s^{0.47}3d^{6.62}$	$d_{xy}^{1.92} + d_{xz}^{0.43} + d_{yz}^{0.82} + d_{x^2-y^2}^{1.56} + d_{z^2}^{1.89}$
Fe(n.n.)-b	0.49	$4s^{0.93}3d^{6.48}$	$d_{xy}^{1.03} + d_{xz}^{1.56} + d_{yz}^{0.96} + d_{x^2-y^2}^{1.41} + d_{z^2}^{1.53}$
As(n.n.n.)	−1.35	$4s^{1.74}4p^{4.74}$	$p_x^{1.51} + p_y^{1.56} + p_z^{1.49}$
As(n.n.n.)	−1.35	$4s^{1.74}4p^{4.74}$	$p_x^{1.51} + p_y^{1.56} + p_z^{1.49}$
		(b) (α-β) spin distribution	
Co	0.98	$4s^{0.01}3d^{0.96}$	$d_{xy}^{0.02} + d_{xz}^{0.00} + d_{yz}^{0.00} + d_{x^2-y^2}^{0.01} + d_{z^2}^{0.93}$
Fe(n.n.)-a	0.01	$4s^{0.00}3d^{0.02}$	$d_{xy}^{0.03} + d_{xz}^{-0.01} + d_{yz}^{-0.01} + d_{x^2-y^2}^{0.01} + d_{z^2}^{0.00}$
Fe(n.n.)-b	−0.28	$4s^{-0.21}3d^{-0.06}$	$d_{xy}^{-0.11} + d_{xz}^{-0.06} + d_{yz}^{0.03} + d_{x^2-y^2}^{0.00} + d_{z^2}^{0.08}$
As(n.n.n.)	−0.02	$4s^{-0.02}4p^{0.00}$	$p_x^{0.02} + p_y^{-0.01} + p_z^{-0.01}$
As(n.n.n.)	−0.02	$4s^{-0.02}4p^{0.00}$	$p_x^{0.02} + p_y^{-0.01} + p_z^{-0.01}$

spin density on the $4p$(As) orbitals. The Co doping induces n.n. and n.n.n. spin transfer and the formation of AFM order. Therefore, the formation mechanism of the magnetic moments seems to be related to a J_1-J_2 AFM Heisenberg model. This model was proposed in [44,45] and used by Poilblanc *et al.* [43] in their study of RVB superconductors; see the discussion in the Introduction.

The superconductor considered in Ref. [43] is characterized by fermionic doped RVB states built of projected singlet pair states on the square lattice. Vacant sites correspond to doped holes (or spinless holons). Let us stress that according to our results presented in Table III, the charge density on the $3d_{yz}$ orbital of Fe-a and Fe-b corresponds to a single electron with practically zero spin density, that is, this electron is spinless. The spin transfer revealed in our study results in the formation of spinless fermions, and it is based on the separability of charge and spin in the nonrelativistic calculations. It is worthwhile to note that the charged spinless holons and chargeless spinons in Anderson's RVB state (see [40–42]) are also based on the separation of charge and spin.

C. The Co-doped cluster in the singlet state

This cluster in the singlet state corresponds to nonmagnetic orthorhombic Co-doped $BaFe_2As_2$, which is SC at low temperature. In this case, we have a restricted calculation; in the two previous cases, the calculations were unrestricted and the spin density was not necessarily the same for each spin direction.

In Table IV, we note an increase of the $3d$ orbital population on the Co atom with respect to the charge observed in the triplet state (see Table III). So, the charge of the Co atom in the nonmagnetic state is less than that in the magnetic-doped material, and it is similar to the charge of the central Fe of the undoped cluster. With respect to the undoped material (Table II), we note an increase of the charge of the Fe atoms and a decrease of the As charges, showing that the Co impurity induces a charge transfer from its Fe neighbors to the As n.n.n.

As in the two previous cases, we find the same group of doubly occupied $3d$(Fe) orbitals associated with a pair of spins of opposite direction, thus with null spin density. We note that for the Co atom, the charge density on the $3d_{x^2-y^2}$ orbital is practically zero. Therefore, this orbital is associated with a vacant electronic state (hole). The other $3d$(Fe) orbitals are partially filled, which means that some of them may correspond to the partially filled $3d$ bands at the Fermi level, as predicted by DFT calculations [17,18] and observed in ARPES experiments [25–27]. The As orbital populations in the singlet state of the Co-doped $Fe_5As_8Ba_4$ cluster present a small decrease with respect to that obtained in the triplet state.

It is worthwhile to note that the charge density of the $3d_{yz}$ orbital of Fe-a and Fe-b and of the $3d_{x^2-y^2}$ orbital of Fe-b corresponds to a single electron, while in the considered singlet state case the spin density on these orbitals (on other orbitals as

TABLE IV. Charge distribution at the MP2 level (NBO analysis) of a Co-doped $Fe_5As_8Ba_4$ cluster ($S = 0$).

	Atomic charge	Valence orbital population	Detailed charge population on $3d$ and $4p$ orbitals
Co	0.85	$4s^{0.47}3d^{7.53}$	$d_{xy}^{1.85} + d_{xz}^{1.73} + d_{yz}^{1.91} + d_{x^2-y^2}^{0.01} + d_{z^2}^{2.02}$
Fe(n.n.)-a	0.82	$4s^{0.48}3d^{6.60}$	$d_{xy}^{2.00} + d_{xz}^{0.31} + d_{yz}^{0.92} + d_{x^2-y^2}^{1.50} + d_{z^2}^{1.85}$
Fe(n.n.)-b	0.60	$4s^{0.80}3d^{6.51}$	$d_{xy}^{1.31} + d_{xz}^{1.67} + d_{yz}^{0.9} + d_{x^2-y^2}^{1.13} + d_{z^2}^{1.50}$
As(n.n.n.)	−1.21	$4s^{1.74}4p^{4.41}$	$p_x^{1.49} + p_y^{1.51} + p_z^{1.40}$
As(n.n.n.)	−1.21	$4s^{1.74}4p^{4.41}$	$p_x^{1.49} + p_y^{1.51} + p_z^{1.41}$

well) is zero. Thus, the null spin density is associated with this electron, and as in the triplet case we have a spinless fermion; see the discussion at the end of the previous subsection.

IV. CONCLUSIONS

Using different multiplicities of the $Fe_5As_8Ba_4$ cluster calculated by the embedded cluster method allowed us to describe several physical situations: pure orthorhombic $BaFe_2As_2$, the high critical temperature SC Co-doped $BaFe_2As_2$ with AFM order or with no magnetism (paramagnetic crystal). In the undoped cluster, the anisotropy in the occupation of $3d_{xz}$ and $3d_{yz}$ orbitals was revealed. This result supports the conception of orbital order that explains anisotropies observed in many experiments.

In the SC case with AFM order, the analysis of orbital population in doped material reveals a spin density increase on the central Co atom with respect to the spin density of the central Fe atom of the undoped case. This increase corresponds mainly to an increase in the $3d_{z^2}$ orbital population of the central atom. The Co doping induces modifications in the spin distribution of the n.n. Fe and n.n.n. As. Therefore, the formation mechanism of the magnetic moment implies n.n. and n.n.n. spin transfer. The formation mechanism of the magnetic moments seems to correspond to a J_1-J_2 AFM Heisenberg model. In nonmagnetic SC material, the magnetic moment on the Co impurity observed in the study of the cluster in the triplet state disappears due to full occupancy of the d_{z^2} orbital; in this case, the Co impurity induces a charge transfer from its n.n. Fe atoms to the n.n.n. As atoms.

It is important to note that some features of the $3d_{yz}$ orbital in the triplet and singlet states of the Co-doped cluster and the $3d_{x^2-y^2}$ orbital in the singlet state of the same cluster can be interpreted as orbitals occupied by a spinless fermion. This result resembles the spinless holon in the Anderson RVB model. Although from this does not follow, a direct applicability of the Anderson RVB theory to our studied iron pnictides; however, there may be some connection between our spinless fermion on some d orbitals of Fe and the "holon" in the fermionic model of the RVB superconductors developed by Poilblanc *et al.* [43]. The possibility of such a connection deserves special study.

ACKNOWLEDGMENTS

The authors acknowledge Luis Fernando Magaña Solis and Juan Ramirez de Arrellano for their assistance during the calculations with the QUANTUM ESPRESSO package; we are grateful to Xim Bokhimi for access to TLALOC clusters. The authors thank the DGTIC computer staff for providing access to the MITZLI clusters of Universidad Nacional Autonoma of Mexico and the support of Universidad de Sonora.

[1] Y. Kamihara, T. Watanabe, M. Hirano, and H. Hosono, J. Am. Chem. Soc. **130**, 3296 (2008).
[2] H. Takahashi, K. Igawa, K. Arii, Y. Kamihara, M. Hirano, H. Hosono, Nature (London) **453**, 376 (2008).
[3] R. G. Stewart, Rev. Mod. Phys. **83**, 1589 (2011).
[4] M. Rotter, M. Tegel, D. Johrendt, I. Schellenberg, W. Hermes, R. Pöttgen, Phys. Rev. B **78**, 020503 (2008).
[5] Q. Huang, Y. Qiu, Wei Bao, M. A. Green, J. W. Lynn, Y. C. Gasparovic, T. Wu, G. Wu, and X. H. Chen, Phys. Rev. Lett. **101**, 257003 (2008).
[6] Y. Su, P. Link, A. Schneidewind, Th. Wolf, P. Adelmann, Y. Xiao, M. Meven, R. Mittal, M. Rotter, D. Johrendt, Th. Brueckel, and M. Loewenhaupt, Phys. Rev. B **79**, 064504 (2009).
[7] M. Liu, L. W. Harriger, H. Luo, M. Wang, R. A. Ewings, T. Guidi, H. Park, K. Haule, G. Kotliar, S. M. Hayden, and P. Dai, Nat. Phys. **8**, 376 (2012).
[8] A. Leithe-Jasper, W. Schnelle, C. Geibel, and H. Rosner, Phys. Rev. Lett **101**, 207004 (2008).
[9] A. S. Sefat, R. Jin, M. A. McGuire, B. C. Sales, D. J. Singh, and D. Mandrus, Phys. Rev. Lett. **101**, 117004 (2008).
[10] Y. Nishikubo, S. Kakiya, M. Danura, K. Kudo, and M. Nohara, J. Phys. Soc. Jpn. **79**, 095002 (2010).
[11] A. S. Sefat, D. J. Singh, L. H. Van Bebber, Y. Mozharivskyj, M. A. McGuire, R. Jin, B. C. Sales, V. Keppens, and D. Mandrus, Phys. Rev. B **79**, 224524 (2009).
[12] A. S. Sefat, K. Marty, A. D. Christianson, B. Saparov, M. A. McGuire, M. D. Lumsden, W. Tian, and B. C. Sales, Phys. Rev. B **85**, 024503 (2012).
[13] Y. Texier, Y. Laplace, P. Mendels, J. T. Park, G. Friemel, D. L. Sun, D. S. Inosov, C. T. Lin, and J. Bobroff, Eur. Phys. Lett. **99**, 17002 (2012).
[14] P. C. Canfield, S. L. Bud'ko, N. Ni, J. Q. Yan, and A. Kracher, Phys. Rev. B **80**, 060501 (2009).
[15] E. D. Mun, S. L. Bud'ko, N. Ni, A. N. Thaler, and P. C. Canfield, Phys. Rev. B **80**, 054517 (2009).
[16] Y. Laplace, J. Bobroff, V. Brouet, G. Collin, F. Rullier-Albenque, D. Colson, and A. Forget, Phys. Rev. B **86**, 020510 (2012).
[17] D. J. Singh and M. H. Du, Phys. Rev. Lett. **100**, 237003 (2008).
[18] I. I. Mazin, D. J. Singh, M. D. Johannes, and M. H. Du, Phys. Rev. Lett. **101**, 057003 (2008).
[19] K. Kuroki, S. Onari, R. Arita, H. Usui, Y. Tanaka, H. Kontani, and H. Aoki, Phys. Rev. Lett. **101**, 087004 (2008).
[20] I. I. Mazin and J. Schmalian, Physica C **469**, 614 (2009).
[21] F. Rullier-Albenque, D. Colson, A. Forget, and H. Alloul, Phys. Rev. Lett. **103**, 057001 (2009).
[22] W. Z. Hu, J. Dong, G. Li, Z. Li, P. Zheng, G. F. Chen, J. L. Luo, and N. L. Wang, Phys. Rev. Lett. **101**, 257005 (2008).
[23] W. Z. Hu, Q. M. Zhang, and N. L. Wang, Physica C **469**, 545 (2009).
[24] D. K. Pratt, M. G. Kim, A. Kreyssig, Y. B. Lee, G. S. Tucker, A. Thaler, W. Tian, J. L. Zarestky, S. L. Bud'ko, P. C. Canfield, B. N. Harmon, A. I. Goldman, and R. J. McQueeney, Phys. Rev. Lett. **106**, 257001 (2011).
[25] V. Brouet, M. F. Jensen, P. H. Lin, A. Taleb-Ibrahimi, P. Le Fèvre, F. Bertran, C. H. Lin, W. Ku, A. Forget, and D. Colson, Phys. Rev. B **86**, 075123 (2012).
[26] Y. Zhang, F. Chen, C. He, B. Zhou, B. P. Xie, C. Fang, W. F. Tsai, X. H. Chen, H. Hayashi, J. Jiang, H. Iwasawa, K. Shimada, H. Namatame, M. Taniguchi, J. P. Hu, and D. L. Feng, Phys. Rev. B **83**, 054510 (2011).

[27] C. Liu, T. Kondo, R. M. Fernandes, A. D. Palczewski, E. D. Mun, N. Ni, A. N. Thaler, A. Bostwick, E. Rotenberg, J. Schmalian, S. L. Bud'ko, P. C. Canfield, and A. Kaminski, Nat. Phys. **6**, 419 (2010).

[28] V. Brouet, M. Marsi, B. Mansart, A. Nicolaou, A. Taleb-Ibrahimi, P. Le Fèvre, F. Bertran, F. Rullier-Albenque, A. Forget, and D. Colson, Phys. Rev. B **80**, 165115 (2009).

[29] P. Vilmercati, A. Fedorov, I. Vobornik, U. Manju, G. Panaccione, A. Goldoni, A. S. Sefat, M. A. McGuire, B. C. Sales, R. Jin, D. Mandrus, D. J. Singh, and N. Mannella, Phys. Rev. B **79**, 220503 (2009).

[30] J. Zhao, W. Ratcliff, J. W. Lynn, G. F. Chen, J. L. Luo, N. L. Wang, J. Hu, and P. Dai, Phys. Rev. B **78**, 140504 (2008).

[31] A. I. Goldman, D. N. Argyriou, B. Ouladdiaf, T. Chatterji, A. Kreyssig, S. Nandi, N. Ni, S. L. Bud'ko, P. C. Canfield, and R. J. McQueeney, Phys. Rev. B **78**, 100506 (2008).

[32] Z. P. Yin and W. E. Pickett, Phys. Rev. B **80**, 144522 (2009).

[33] F. Wang and D.-H. Lee, Science **332**, 200 (2011)

[34] M. R. Norman, Science **332**, 196 (2011).

[35] Q. M. Si and E. Abrahams, Phys. Rev. Lett. **101**, 076401 (2008).

[36] K. Seo, B. A. Bernevig, and J. P. Hu, Phys. Rev. Lett. **101**, 206404 (2008).

[37] W.-Q. Chen, K.-Y. Yang, Y. Zhou, and F.-C. Zhang, Phys. Rev. Lett. **102**, 047006 (2009).

[38] P. A. Lee, N. Nagaosa, and X.-G. Wen, Rev. Mod. Phys. **78**, 17 (2006).

[39] P. W. Anderson, Science **235**, 1196 (1987).

[40] S. A. Kivelson, D. S. Rokhsar, and J. P. Sethna, Phys. Rev. B **35**, 8865 (1987).

[41] P. W. Anderson, G. Baskaran, Z. Zou, and T. Hsu, Phys. Rev. Lett. **58**, 2790 (1987).

[42] P. W. Anderson and R. Schrieffer, Phys. Today **44**(6), 54 (1991).

[43] D. Poilblanc, Ph. Corboz, N. Schuch, and J. I. Cirac, Phys. Rev. B **89**, 241106 (2014).

[44] P. Gosvami, R. Yu, Q. Si, and E. Abrahams, Phys. Rev. B **84**, 155108 (2011).

[45] D. X. Yao and E. W. Carlson, Phys. Rev. B **78**, 052507 (2008).

[46] K. W. Kim, A. Pashkin, H. Schäfer, M. Beyer, M. Porer, T. Wolf, C. Bernhard, J. Demsar, R. Huber, and A. Leitenstorfer, Nat. Mater. **11**, 497 (2012).

[47] M. G. Kim, R. M. Fernandes, A. Kreyssig, J. W. Kim, A. Thaler, S. L. Bud'ko, P. C. Canfield, R. J. McQueeney, J. Schmalian, and A. I. Goldman, Phys. Rev. B **83**, 134522 (2011).

[48] S. Nandi, M. G. Kim, A. Kreyssig, R. M. Fernandes, D. K. Pratt, A. Thaler, N. Ni, S. L. Bud'ko, P. C. Canfield, J. Schmalian, R. J. McQueeney, and A. I. Goldman, Phys. Rev. Lett. **104**, 057006 (2010).

[49] L. Baldassarre, A. Perucchi, P. Postorino, S. Lupi, C. Marini, L. Malavasi, J. Jiang, J. D. Weiss, E. E. Hellstrom, I. Pallecchi, and P. Dore, Phys. Rev B **85**, 174522 (2012).

[50] A. A. Schafgans, S. J. Moon, B. C. Pursley, A. D. LaForge, M. M. Qazilbash, A. S. Sefat, D. Mandrus, K. Haule, G. Kotliar, and D. N. Basov, Phys. Rev. Lett. **108**, 147002 (2012).

[51] A. Georges, L. de' Medici, and J. Mravlje, Annu. Rev. Condens. Matter Phys. **4**, 137 (2013).

[52] D. N. Basov, R. D. Averitt, D. van der Marel, M. Dressel, and K. Haule, Rev. Mod. Phys. **83**, 471 (2011).

[53] N. Ni, M. E. Tillman, J.-Q. Yan, A. Kracher, S. T. Hannahs, S. L. Bud'ko, and P. C. Canfield, Phys. Rev. B **78**, 214515 (2008).

[54] W. Pickett, Nat. Phys. **5**, 87 (2009).

[55] R. M. Fernandes, E. Abrahams, and J. Schmalian, Phys. Rev. Lett. **107**, 217002 (2011).

[56] C. Lester, J.-H. Chu, J. G. Analytis, S. C. Capelli, A. S. Erickson, C. L. Condron, M. F. Toney, I. R. Fisher, and S. M. Hayden, Phys. Rev. B **79**, 144523 (2009).

[57] D. K. Pratt, W. Tian, A. Kreyssig, J. L. Zarestky, S. Nandi, N. Ni, S. L. Bud'ko, P. C. Canfield, A. I. Goldman, and R. J. McQueeney, Phys. Rev. Lett. **103**, 087001 (2009).

[58] R. M. Fernandes, S. Maiti, P. Wölfle, and A. V. Chubukov, Phys. Rev. Lett. **111**, 057001 (2013).

[59] I. G. Kaplan, J. Soullard, J. Hernandez-Cobos, and R. Pandey, J. Phys.: Condens. Matter **11**, 1049 (1999).

[60] I. G. Kaplan, J. Hernandez-Cobos, and J. Soullard, *Quantum Systems in Chemistry and Physics* (Kluwer Academic, Dordrecht, 2000), Vol. 1, pp. 143–158.

[61] I. G. Kaplan and J. Soullard, Int. J. Quantum Chem. **80**, 320 (2000).

[62] I. G. Kaplan, J. Soullard, and J. Hernandez-Cobos, Phys. Rev. B **65**, 214509 (2002).

[63] I. G. Kaplan, *Intermolecular Interactions: Physical Picture, Computational Methods and Model Potentials* (Wiley, Chichester, 2006).

[64] J. M. Vail, *Topics in the Theory of Solid Materials* (Institute of Physics, Bristol, 2003).

[65] P. Giannozzi *et al.*, J. Phys.: Condens. Matter **21**, 395502 (2009).

[66] P. Giannozzi *et al.*, arXiv:0906.2569

[67] M. J. Frisch *et al.*, *Gaussian 09, Revision C.01* (Gaussian Inc., Pittsburgh, 2009).

[68] C.-C. Chen, J. Maciejko, A. P. Sorini, B. Moritz, R. R. P. Singh, and T. P. Devereaux, Phys. Rev. B **82**, 100504(R) (2010).

[69] W. Lv and P. Phillips, Phys. Rev. B **84**, 174512 (2011).

[70] T. Saito, S. Onari, and H. Kontani, Phys. Rev. B **82**, 144510 (2010).

[71] C.-C. Lee, W.-G. Yin, and W. Ku, Phys. Rev. Lett. **103**, 267001 (2009).

[72] M. A. Tanatar, A. Kreyssig, S. Nandi, N. Ni, S. L. Budko, P. C. Canfield, A. I. Goldman, and R. Prozorov, Phys. Rev. B **79**, 180508 (2009).

[73] M. Nakajima, T. Liang, S. Ishida, Y. Tomioka, K. Kihou, C. H. Lee, A. Iyo, H. Eisaki, T. Kakeshita, T. Ito, and S. Uchida, Proc. Natl. Acad. Sci. (USA) **108**, 12238 (2011).

[74] S. Ishida, M. Nakajima, T. Liang, K. Kihou, C. H. Lee, A. Iyo, H. Eisaki, T. Kakeshita, Y. Tomioka, T. Ito, and S. Uchida, Phys. Rev. Lett. **110**, 207001 (2013); J. Am. Chem. Soc. **135**, 3158 (2013).

[75] J.-H. Chu, J. G. Analytis, K. De Greve, P. L. McMahon, Z. Islam, Y. Yamamoto, and I. R. Fisher, Science **329**, 824 (2010).

[76] J.-H. Chu, H.-H. Kuo, J. G. Analytis, and I. R. Fisher, Science **337**, 710 (2012).

[77] Y. K. Kim, H. Oh, C. Kim, D. Song, W. Jung, B. Kim, H. J. Choi, C. Kim, B. Lee, S. Khim, H. Kim, K. Kim, J. Hong, and Y. Kwon, Phys. Rev. B **83**, 064509 (2011).

[78] M. Yi, D. Lu, J.-H. Chu, J. G. Analytis, A. P. Sorini, A. F. Kemper, B. Moritz, S.-K. Mo, R. G. Moore, M. Hashimoto, W.-S. Lee, Z. Hussain, T. P. Devereaux, I. R. Fisher, and Z.-X. Shen, Proc. Natl. Acad. Sci. (USA) **108**, 6878 (2011).

[79] I. R. Fisher, L. Degiorgi, and Z. X. Shen, Rep. Prog. Phys. **74**, 124506 (2011); C. Fang, H. Yao, W.-F. Tsai, J. Hu, and S. A. Kivelson, Phys. Rev. B **77**, 224509 (2008).

[80] M. N. Gastiasoro, P. J. Hirschfeld, and B. M. Andersen, Phys. Rev. B **89**, 100502 (2014).

[81] J.-H. Chu, J. G. Analytis, C. Kucharczyk, and I. R. Fisher, Phys. Rev B **79**, 014506 (2009).